Expanded View Figures

Figure EV1. IFNAR1-independent potentiation of nucleic acid sensors by translation inhibition.

A IFN-β production was measured by ELISA in cell culture supernatants of WT and PKR$^{-/-}$ MEFs that were stimulated with HMW poly(I:C) for 4 and 8 h. Results are the mean ± SD of three independent experiments.

B PKR$^{-/-}$ MEFs were left untreated (NT) or were treated with HMW or LMW poly(I:C) for 8 h in the presence or not of 5 μg/ml of cycloheximide (CHX). ATF4 and phospho-IRF3 levels in nuclear extracts were detected by immunoblot. β-actin was used as equal loading control. WT MEFs were treated with LMW poly(I:C) for 4 h and the corresponding nuclear extract was used as a positive control for ATF4 detection.

C WT MEFs were lipofected with poly(I:C) (green) or cGAMP (pink) for the indicated time in the presence or absence of CHX. Cells were pulsed with puromycin prior to collection, staining with anti-puromycin and anti-pTBK1 and flow cytometry analysis. Quantification is presented as histograms on the right ($n \geq 2$). Bars are mean ± SD.

D IFNAR1$^{-/-}$ MEFs were lipofected with poly(I:C) for the indicated time in the presence (shades of blue) or absence (shades of red) of CHX. Cells were pulsed with puromycin prior to collection, staining with anti-puromycin and anti-pTBK1, and flow cytometry analysis.

E IFNAR1$^{-/-}$ MEFs were lipofected with poly(I:C) for the indicated time in the presence or absence of CHX. Cells were pulsed with puromycin prior to collection and immunoblot detection of puromycin and SHIP-1. β-actin was used as equal loading control. Quantification of the blot is presented below.

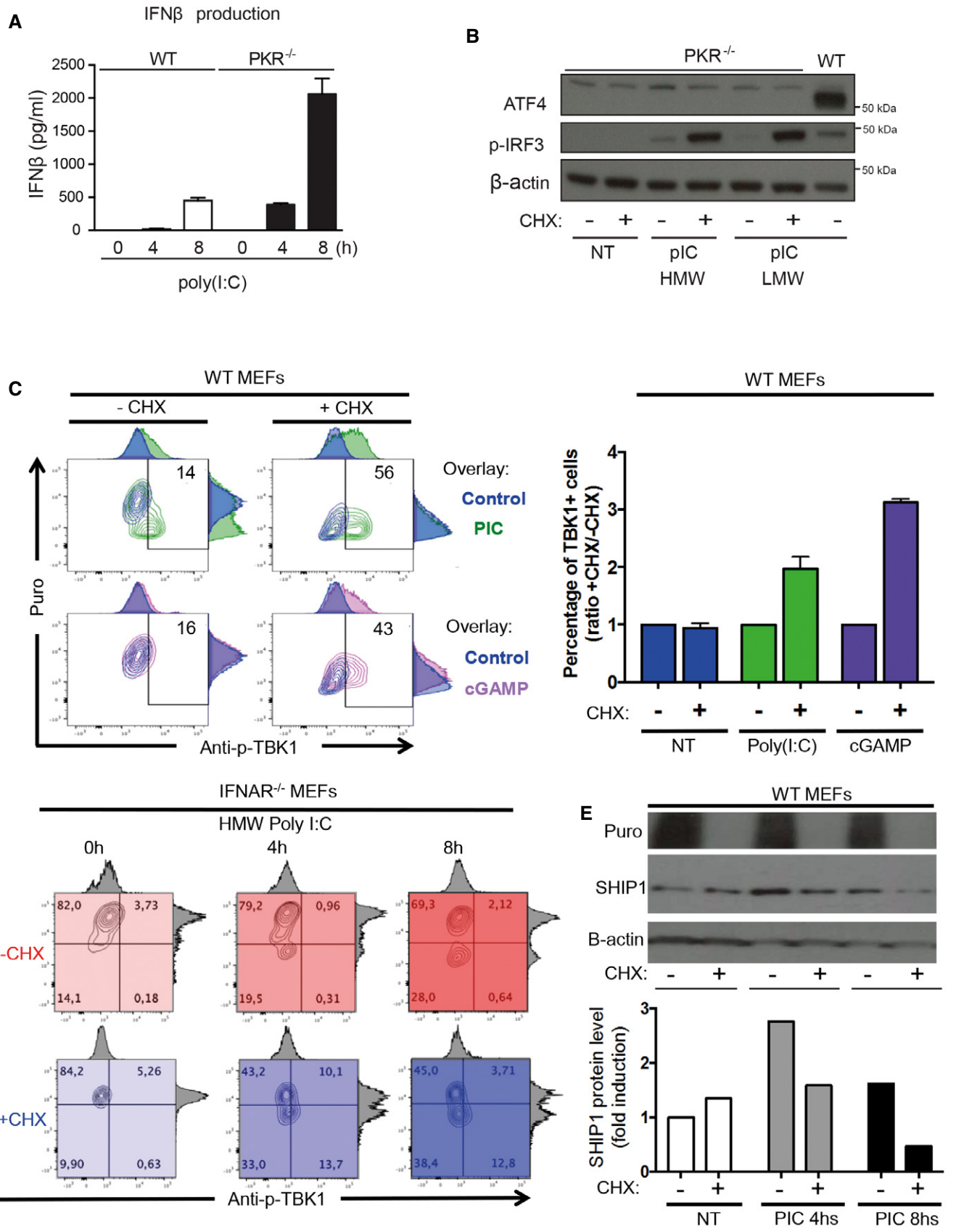

Figure EV1.

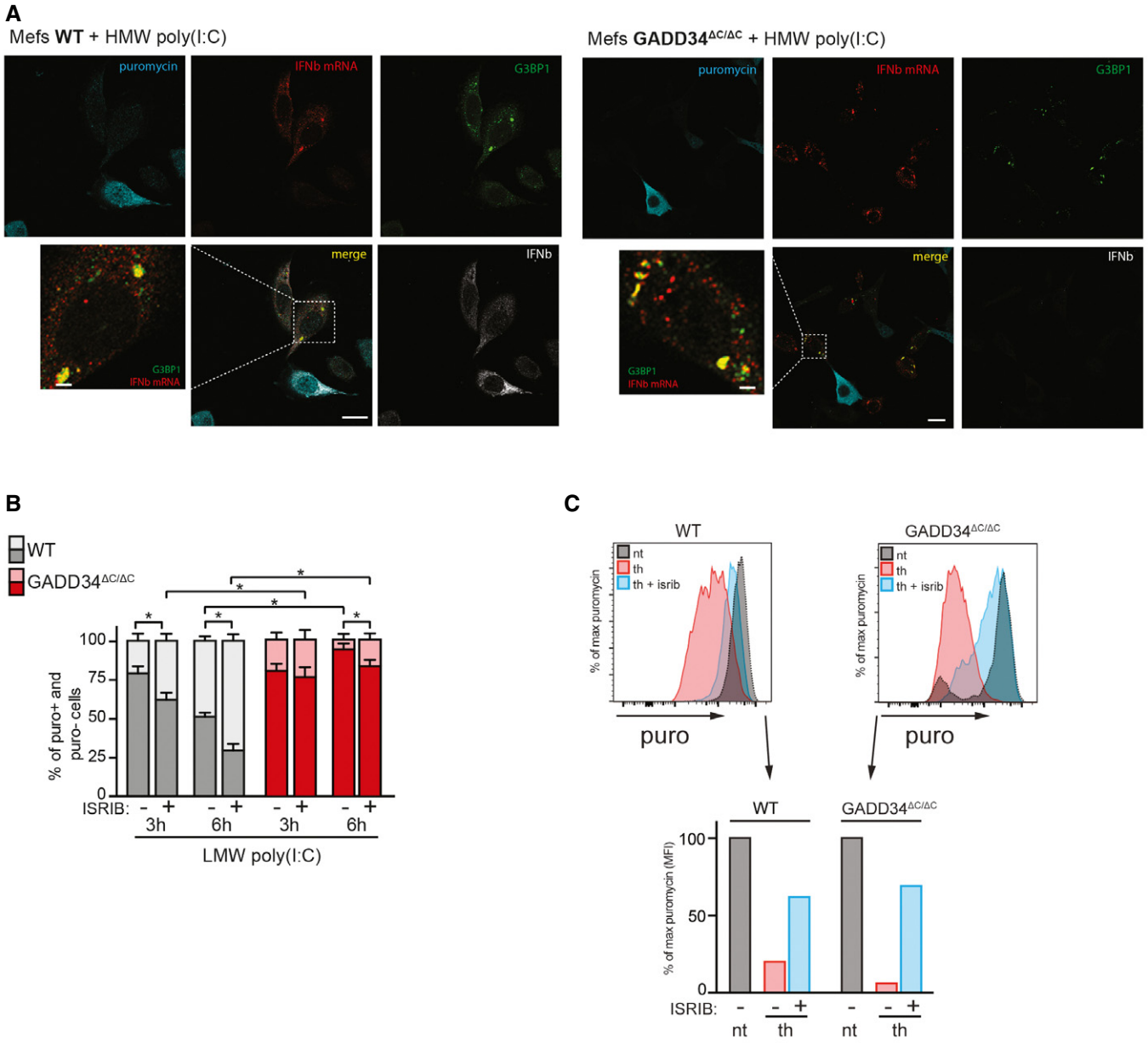

Figure EV2. Level of total translation, IFN production and IFN mRNA in WT and KO upon dsRNA stimulation.

A Fluorescence *in situ* hybridization (FISH) for *IFNB* mRNA, combined with immunofluorescence staining for protein synthesis (with an anti-puromycin mAb), for stress granules (with anti-G3BP1 Ab) and for IFN-β protein in WT and GADD34$^{\Delta C/\Delta C}$ MEFs stimulated with HMW poly(I:C) for 6 h and labeled with puromycin for 10 min. Scale bars = 10 μm.

B WT and GADD34$^{\Delta C/\Delta C}$ MEFs were stimulated with LMW poly(I:C) for indicated times in the presence of ISRIB and puromycin for protein synthesis measurement by FACS. Percentiles of translating (puro^{+}, light color) and non-translating cells (puro^{-}, dark color) were determined by flow cytometry from fluorescence intensity of individual cells and are represented as cumulative bars for WT (gray) and GADD34$^{\Delta C/\Delta C}$ MEFs (red). *P*-values were calculated using a Student's *t*-test, *$P < 0.05$. Mean ± SD.

C Similar experiments were conducted with thapsigargin and ISRIB. In UPR conditions, ISRIB rescued protein synthesis efficiently, confirming the efficacy of the drug on this pathway. Although ISRIB abrogates the impact of eIF2α phosphorylation on translation initiation during ER stress, it does not efficiently restore protein synthesis and cytokines production in cells responding to dsRNA.

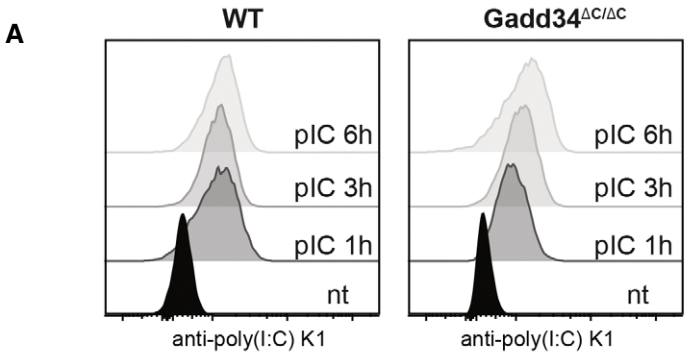

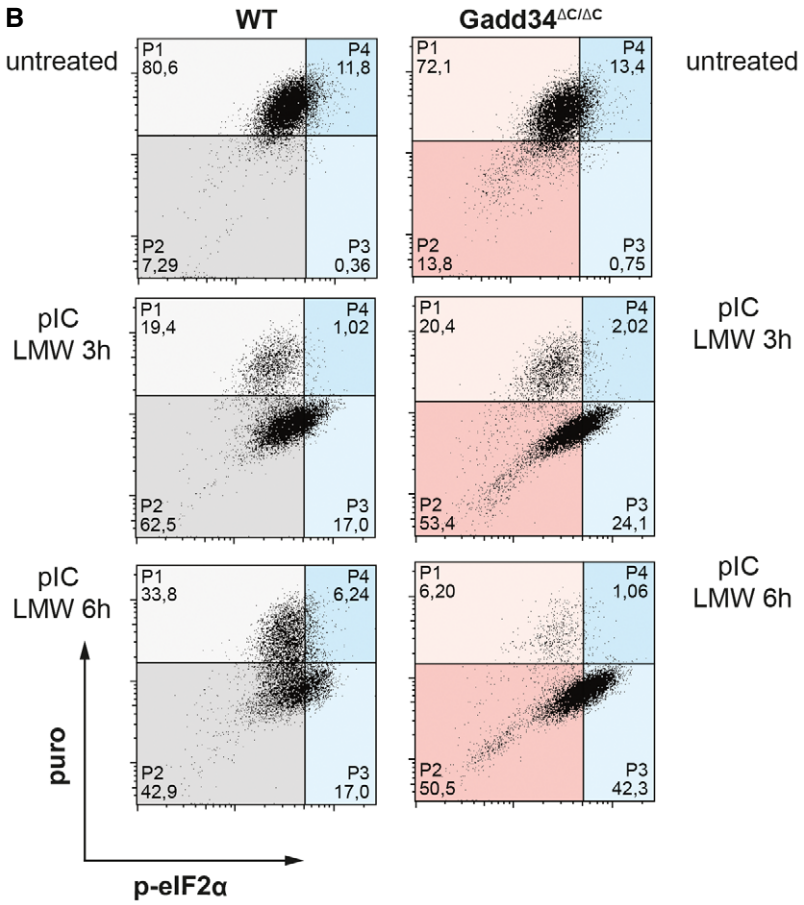

Figure EV3. Levels of intracellular poly(I:C) uptake and eIF2α phosphorylation in WT and GADD34$^{\Delta C/\Delta C}$ MEFs.

A WT and GADD34$^{\Delta C/\Delta C}$ MEFs were treated with poly(I:C) for 1, 3, and 6 h before fixation and permeabilization. Poly(I:C) was detected with specific K1 mAb using intracellular flow cytometry.

B Two-dimensional plots of fluorescence intensity of individual WT (grey and blue) and GADD34$^{\Delta C/\Delta C}$ MEFs (red and blue) stained for puromycin (*y*-axis) and p-eIF2α (*x*-axis). Percentage of cells in each quadrant is indicated. Cells expressing p-eIF2α are shifted in the two right quadrants (P3 and P4, blue).

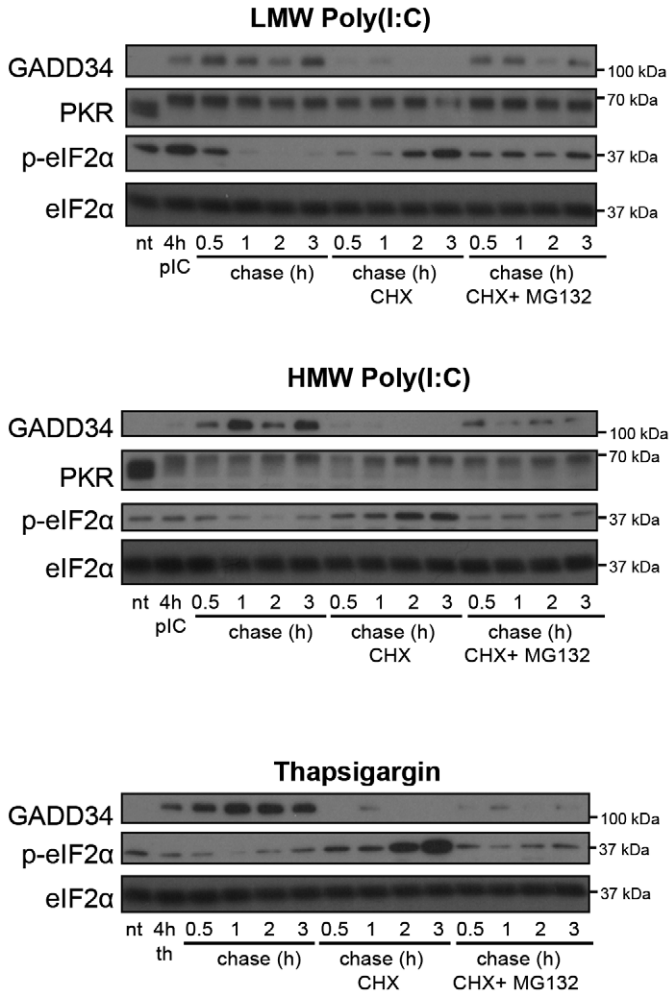

Figure EV4. GADD34 half-life upon poly(I:C) treatment.

WT MEFs were treated with HMW poly(I:C), LMW poly (I:C), or thapsigargin (th) for 4 h, prior to a chase of 0.5, 1, 2, and 3 h with fresh medium. When indicated, cycloheximide (CHX) +/− MG132 were added to the medium during the chase. GADD34, PKR, p-eIF2α, and total eIF2α were detected by immunoblot with specific antibodies.

Figure EV5. Mathematical modeling of protein synthesis oscillation upon increased GADD34 half-life and reduced parameters variability.

A Schematic representation of the biochemical relationships and interdependences used to establish the mathematical model described in the Materials and Methods section. For this simulation, parameter C3 of equation 7 and parameter C2 of equation 6 were decreased by 30% and parameter C4 of equation 7 by 10%, while random variability was kept at 10%.

B Graphic representation over time of model-based levels of p-eIF2α (red), protein synthesis (black), and GADD34 activity (blue), demonstrating the more rapid oscillatory nature of protein synthesis with these modified parameters.

C Representative single-cell simulation showing the progression across quadrants (P1–P4) representing protein synthesis intensity and GADD34 levels over time (rainbow color gradient). Cells undergo more rapid and compact cycles of protein synthesis inhibition and rescue.

D Grouped simulations of 200 cells over 450 time steps. By introducing 10% of variability in most parameters with fixed delays, virtual cell behavior mimics closely the experimental situation observed in Fig 5D. Few dead cells are represented in red and subtracted from the indicated cell percentiles in each quadrant.

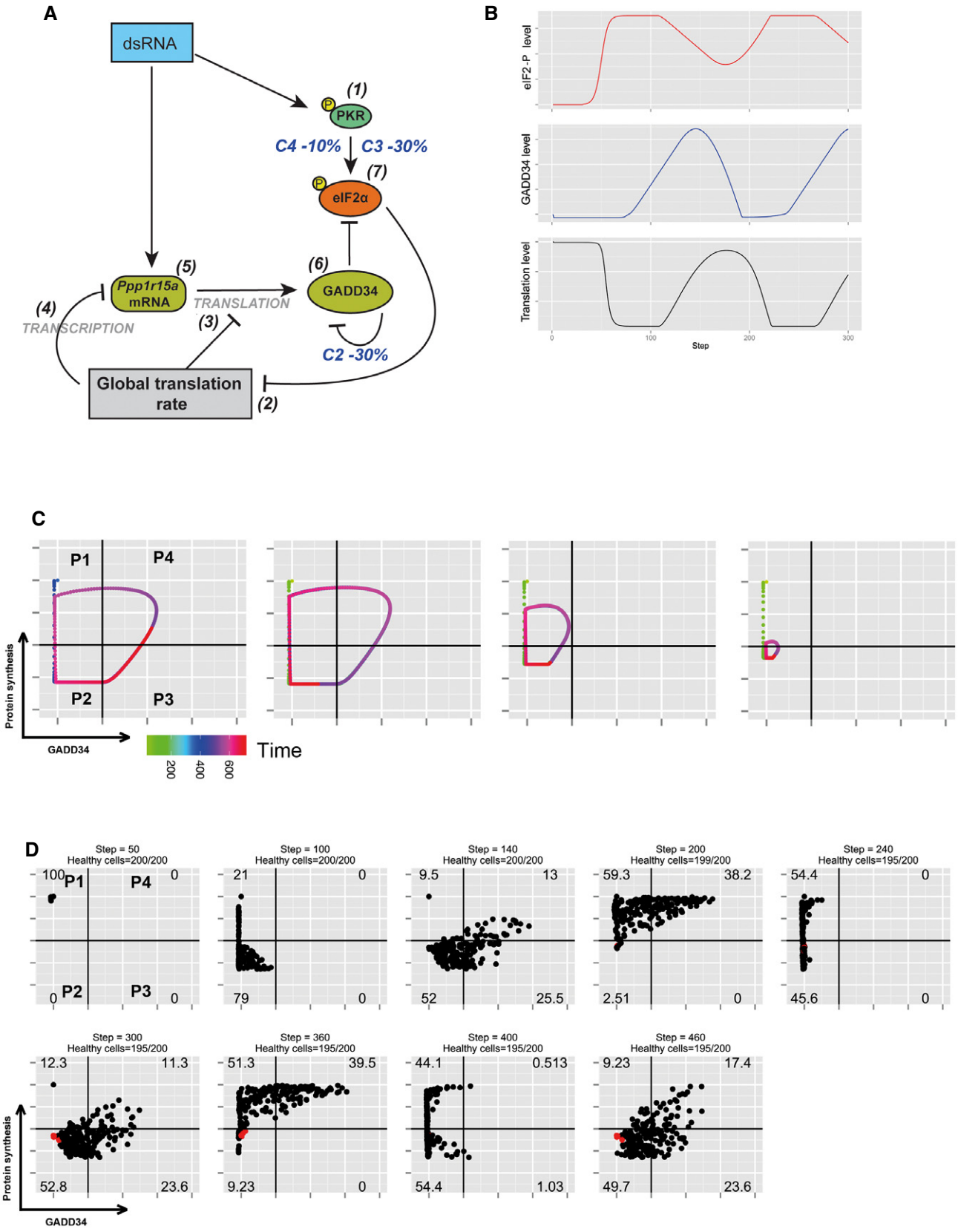

Figure EV5.